

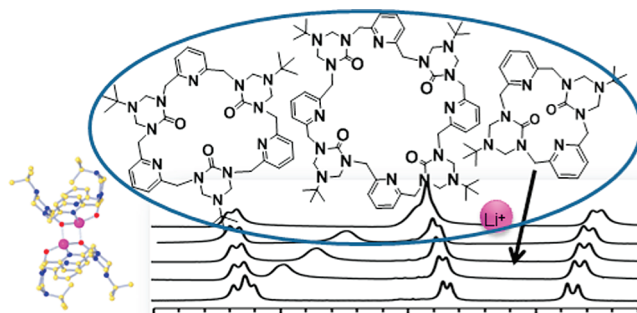
## Alkali Metal Ions As Probes of Structure and Recognition Properties of Macrocyclic Pyridyl Urea Hosts

Kinkini Roy, Chun Wang, Mark D. Smith, Perry J. Pellechia, and Linda S. Shimizu\*

Department of Chemistry and Biochemistry, University of South Carolina, Columbia, South Carolina 29208

shimizul@chem.sc.edu

Received May 14, 2010



We report the one-pot synthesis of three symmetrical macrocyclic pyridyl urea hosts. X-ray crystal studies were used to confirm the structures of the free hosts and their host·guest complexes with alkali metal ions. These solid-state studies revealed the interactions that were important for binding cations ( $\text{Li}^+$ ,  $\text{Na}^+$ , and  $\text{K}^+$ ). The affinity of these hosts for alkali metal salts were evaluated in solution ( $\text{CD}_3\text{CN}$ ), and the stoichiometries of the solution complexes were compared with their solid-state structures. Two of these hosts showed high affinity for  $\text{LiBF}_4$ , which was primarily due to strong interactions between the urea oxygens and the cations with pyridine nitrogens contributing additional stabilizing interactions.

### Introduction

In the past two decades, chemists have made tremendous progress in supramolecular assembly and can now predictably design self-assembly systems based on weak noncovalent interactions including metal–ligand interactions,<sup>1</sup> hydrogen bonds (H-bonds),<sup>2</sup>  $\pi$ – $\pi$  interactions,<sup>3</sup> ion–dipole interactions,<sup>4</sup> and hydrophobic interactions.<sup>5</sup> What has been more challenging has been to mimic the types of complex functional assemblies found in nature that are capable of catalysis, sensing, motion, and replication. The difficulty is in designing multifunctional systems in which one set of functional groups is responsible for the assembly and structure

formation and the second set of functional groups is responsible for function.<sup>6</sup> For example, an enzyme contains groups that govern its folding and a second set of groups for recognition and catalysis. Often, similar groups are used for both jobs, and the challenge is to selectively program these groups to carry out their appointed tasks.

Our specific interest has been in incorporating catalytic and recognition groups into the interiors of our self-assembling urea macrocycles. Typical rigid bis-urea macrocycles, such as phenyl ether **1**, assembled into columns through strong three-centered urea self-association and aryl-stacking interactions (Figure 1).<sup>7</sup> In our next generation of self-assembling bis-urea macrocycles, we want to design the system to include new interior functional groups (R groups in Figure 1) that are orthogonal in orientation and purpose

(1) (a) Caulder, D. L.; Raymond, K. N. *J. Chem. Soc., Dalton Trans.* **1999**, 1185–1200. (b) Leininger, S.; Olenyuk, B.; Stang, P. *J. Chem. Rev.* **2000**, *100*, 853–907. (c) Nitschke, J. R. *Acc. Chem. Res.* **2007**, *40*, 103–112.

(2) Prins, L. J.; Reinhoudt, D. N.; Timmerman, P. *Angew. Chem., Int. Ed.* **2001**, *40*, 2382–2426.

(3) (a) Meyer, E. A.; Castellano, R. K.; Diederich, F. *Angew. Chem., Int. Ed.* **2003**, *42*, 1210–1250. (b) Lee, E. C.; Kim, D.; Jurecka, P.; Tarakeshwar, P.; Hobza, P.; Kim, K. S. *J. Phys. Chem. A* **2007**, *111*, 3446–3457.

(4) (a) Davis, J. T.; Spada, G. P. *Chem. Soc. Rev.* **2007**, *36*, 296–313. (b) Hosseini, M. W. *Coord. Chem. Rev.* **2003**, *240*, 157–166.

(5) (a) Blokzijl, W.; Engberts, J. B. F. N. *Angew. Chem., Int. Ed.* **1993**, *32*, 1545–1579. (b) Rekharsky, M.; Inoue, Y. *Chem. Rev.* **1998**, *98*, 1875–1917.

(6) (a) Vriezema, D. M.; Aragones, M. C.; Elemans, J. A. A. W.; Cornelissen, J. J. L. M.; Rowan, A. E.; Nolte, R. J. M. *Chem. Rev.* **2005**, *105*, 1445–1489. (b) Koblenz, T. S.; Wassenaar, J.; Reek, J. N. H. *Chem. Soc. Rev.* **2008**, *37*, 247–262.

(7) (a) Shimizu, L. S.; Hughes, A. D.; Smith, M. D.; Davis, M. J.; Zhang, P.; zur Loye, H. –C.; Shimizu, K. D. *J. Am. Chem. Soc.* **2003**, *125*, 14972–14973. (b) Dewal, M. B.; Lufaso, M. W.; Hughes, A. D.; Samuel, S. A.; Pellechia, P.; Shimizu, L. S. *Chem. Mater.* **2006**, *18*, 4855–4864.

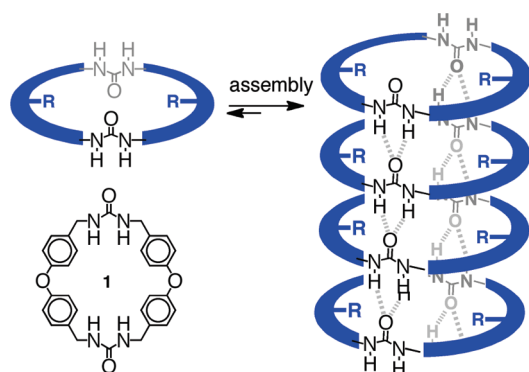


**FIGURE 1.** Schematic assembly of bis-urea macrocycles containing interior functional groups (R groups). Current rigid bis-urea macrocycles such as phenyl ether **1** contain no functional groups that protrude into the interior cavity. These macrocycles assembled into columns through urea hydrogen bonds and aryl-stacking interactions.

to the urea groups. These groups should not interfere with the urea–urea interactions that guide the formation of the columnar assemblies. We report, herein, our initial design and studies of multifunctional macrocycles that contain urea and pyridine groups, potential competitors for H bonds. We investigated the structure and molecular recognition properties of the soluble unassembled hosts to probe how the two functional groups interacted. By studying the complexation of simple alkali salts, we were able to examine the relative importance of these two types of sites (pyridine nitrogen versus the urea oxygen) for complex formation. These studies allowed comparison of the relative affinities of these two functional groups for cations and provided information about the potential compatibility of these groups within this supramolecular assembly motif.

Ureas and pyridines are important for catalysis and molecular recognition. Ureas display selective interactions with cations due to their highly polarized carbonyl groups. Macrocyclic hosts that incorporate ureas are known to complex alkali metal cations with high association constants.<sup>8</sup> Hosts with polyaza functionalities are also known

to possess powerful ligating abilities toward metal ions and have been incorporated into artificial receptors<sup>9</sup> and ion sensors.<sup>10</sup> Even aromatic nitrogens can be important for forming interaction with cations, and fluorescent 1,10-phenanthroline derivatives have been shown to be selective sensors for lithium ions.<sup>11</sup> Some systems combined these two functional groups into host structures and compare the primary interactions that contribute to complex formation. Literature work on spherands that include both aza and urea functionalities<sup>12</sup> and linear oligomers of pyridine/imidazolidin-2-one<sup>13</sup> suggested that the urea carbonyl oxygens were responsible for the primary interactions with cations. Indeed, crystalline complexes of aromatic nitrogen bases and simple group 1 metal salts are known,<sup>14</sup> although water can displace some of the nitrogen base from these cations.<sup>15</sup> Given literature precedence, we decided to utilize alkali metal cations as a means to probe the ligating ability of pyridines and ureas that are in close proximity within our macrocyclic framework.

Ureas are readily synthesized and have a high propensity to assemble; however, they typically have low solubility that can complicate systematic evaluation of their properties. Removal of the urea NHs by triazinanone formation increased the solubility of these macrocycles by preventing their assembly and enabled the investigation of the molecular recognition properties of these macrocycles in solution. We synthesized triazinanone-protected urea and pyridine hosts **2–4** via a one-pot synthesis (Scheme 1). The tendency of the triazinanone macrocycles and their alkali metal complexes to form crystals was particularly advantageous as it enabled examination of their solid-state structures via X-ray crystallography. These solid-state studies elucidated the interactions that were important for cation binding. Many of the forces that contribute to the complexation of alkali metal cations such as the directing of the heteroatom lone pairs toward the cation or ion–dipole interactions (electrostatics)<sup>16</sup> within these hosts are also important when considering the H-bond acceptor ability of ureas and pyridines. Cations do have preferences in terms of polarizability (“hard” vs “soft”) and oxophilicity or azophilicity. The “hard” alkali metal cations often prefer hard Lewis bases, although they have been shown to form strong interactions

(8) (a) Hayward, R. J.; Meth-Cohn, O. *J. Chem. Soc., Perkin Trans. 1* **1975**, 212–219. (b) Nolte, R. J. M.; Cram, D. J. *J. Am. Chem. Soc.* **1984**, *106*, 1416–1420. (c) Cram, D. J.; Dicker, I. B.; Lauer, M.; Knobler, C. B.; Trueblood, K. N. *J. Am. Chem. Soc.* **1984**, *106*, 7150–7167. (d) Bryant, J. A.; Ho, S. P.; Knobler, C. B.; Cram, D. J. *J. Am. Chem. Soc.* **1990**, *112*, 5837–5843. (e) Smeets, J. W. H.; Sijbesma, R. P.; van Dalen, L.; Spek, A. L.; Smeets, W. J. J.; Nolte, R. J. M. *J. Org. Chem.* **1989**, *54*, 3710–3717. (f) Smeets, J. W. H.; van Dalen, L.; Kaats-Richter, V. E. M.; Nolte, R. J. M. *J. Org. Chem.* **1990**, *55*, 454–461. (g) Cram, D. J.; Katz, H. E.; Dicker, I. B. *J. Am. Chem. Soc.* **1984**, *106*, 4987–5000. (h) Kumar, S.; Saini, R.; Singh, H. *Tetrahedron Lett.* **1992**, *32*, 7937–7940. (i) Kilburn, J. D.; MacKenzie, A. R.; Still, W. C. *J. Am. Chem. Soc.* **1988**, *110*, 1307–1308. (j) Rosser, M.; Parker, D.; Ferguson, G.; Gallagher, J. F.; Howard, J. A. K.; Yufit, D. S. *Chem. Commun.* **1993**, 1267–1269. (k) Chapoteau, E.; Chowdhary, M. S.; Czech, B. P.; Kumar, A.; Zazulak, W. J. *J. Org. Chem.* **1992**, *57*, 2804–2808. (l) Chen, J.-A.; Lai, J.-L.; Lee, G. H.; Wang, Y.; Su, J. K.; Yeh, H.-C.; Lin, W.-Y.; Leung, M. *Org. Lett.* **2001**, *3*, 3999–4002.

(9) (a) Nitschke, J. R.; Tilley, T. D. *Angew. Chem., Int. Ed.* **2001**, *40*, 2142–2145. (b) Henze, O.; Lentz, D.; Schluter, A. D. *Chem.—Eur. J.* **2000**, *6*, 2362–2367. (c) Tobe, Y.; Nagano, A.; Kawabata, K.; Sonoda, M.; Naemura, K. *Org. Lett.* **2000**, *2*, 3265–3268. (d) Droz, A. S.; Neidlein, U.; Anderson, S.; Seiler, P.; Diederich, F. *Helv. Chim. Acta* **2001**, *84*, 2243–2289. (e) Grauer, A.; Riechers, A.; Ritter, S.; König, B. *Chem.—Eur. J.* **2008**, *14*, 8922–8927. (f) Rivera, D. B.; Pando, O.; Bosch, F.; Wessjohann, L. A. *J. Org. Chem.* **2008**, *73*, 6229–6238.

(10) (a) Baxter, P. N. W. *J. Org. Chem.* **2001**, *66*, 4170–4179. (b) Baxter, P. N. W. *Chem.—Eur. J.* **2002**, *8*, 5250–5264.

(11) (a) Obare, S. O.; Murphy, C. J. *Inorg. Chem.* **2001**, *40*, 6080–6082. (b) Sugihara, H.; Okada, T.; Hiratani, K. *Anal. Sci.* **1993**, *9*, 593–597. (c) Hiratani, K.; Nomoto, M.; Sugihara, H.; Okada, T. *Analyst* **1992**, *117*, 1491–1495. (d) Okada, T.; Sugihara, H.; Hiratani, K. *Analyst* **1995**, *120*, 2381–2386.

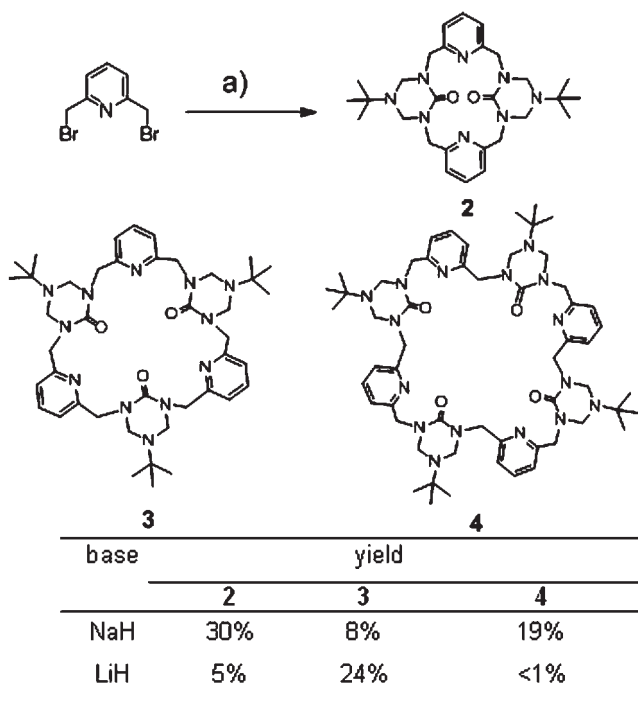
(12) Katz, H. E.; Cram, D. J. *J. Am. Chem. Soc.* **1984**, *106*, 4977–4987.

(13) Meth-Cohn, O.; Yan, Z. *J. Chem. Soc., Perkins Trans. 1* **1998**, 423–436.

(14) (a) Buttery, J. H. N.; Effendy; Mutfroin, S.; Plackett, N. C.; Skelton, B. W.; Whitaker, C. R.; White, A. H. *Z. Anorg. Allg. Chem.* **2006**, *632*, 1809–1828. (b) Buttery, J. H. N.; Effendy; Koutsantonis, G. A.; Mutfroin, S.; Plackett, N. C.; Skelton, B. W.; Whitaker, C. R.; White, A. H. *Z. Anorg. Allg. Chem.* **2006**, *632*, 1829–1838. (c) Buttery, J. H. N.; Effendy; Mutfroin, S.; Plackett, N. C.; Skelton, B. W.; Somers, N.; Whitaker, C. R.; White, A. H. *Z. Anorg. Allg. Chem.* **2006**, *632*, 1838–1859. (d) Buttery, J. H. N.; Effendy; Mutfroin, S.; Plackett, N. C.; Skelton, B. W.; Whitaker, C. R.; White, A. H. *Z. Anorg. Allg. Chem.* **2006**, *632*, 1851–1855.

(15) (a) Raston, C. L.; Skelton, B. W.; Whitaker, C. R.; White, A. H. *Aust. J. Chem.* **1988**, *41*, 409–412. (b) Raston, C. L.; Whitaker, C. R.; White, A. H. *Aust. J. Chem.* **1988**, *41*, 823–826. (c) Raston, C. L.; Whitaker, C. R.; White, A. H. *Aust. J. Chem.* **1988**, *41*, 413–416. (d) Weiss, E. *Angew. Chem., Int. Ed.* **1993**, *32*, 1501–1523.

(16) (a) Izatt, R. M.; Bradshaw, J. S.; Nielsen, S. A.; Lamb, J. D.; Christensen, J. J. *Chem. Rev.* **1985**, *85*, 271–339. (b) Pedersen, C. J.; Frensdor, H. K. *Angew. Chem., Int. Ed.* **1972**, *11*, 16–25.

SCHEME 1. Synthesis of Pyridyl Macrocycles 2–4.<sup>a</sup>

<sup>a</sup>Reagents and conditions: (a) triazinanone (2.5 mM in THF), base, 80 °C (1 h), cooling, followed by dropwise addition of dibromide (1.2 mM in THF), 48 h.

with both ureas and pyridines, which are both more polarizable.<sup>8–13</sup>

## Results and Discussion

The hosts were synthesized in a one-pot procedure from the macrocyclization of 2,6-bis(bromomethyl)pyridine and triazinanone<sup>17</sup> under basic conditions (NaH) in anhydrous THF (Scheme 1). After aqueous workup, the mixture was separated by column chromatography to afford the three symmetrical macrocyclic hosts **2** (30%), **3** (8%), and **4** (19%) and open-chain oligomers. The yields of the pyridine and urea macrocycles were considerably higher than those of the analogous benzene-urea macrocycles.<sup>18</sup> The higher yields and the isolation of different sized macrocyclic products in the pyridyl case suggested we might be able to use a template to increase the yield and selectivity of the macrocyclization step. Therefore, we investigated the use of other bases for this reaction. Use of lithium hydride afforded a different product ratio with trimer **3** as the major product (24%) and dimer **2** (5%) as a side product with 32% recovery of the dibromide after 3 days. Longer reaction times and excess base gave similar conversions. The different product distributions with different base cations (Li<sup>+</sup> vs Na<sup>+</sup>) provided the first evidence that host **3** could bind lithium.

Due to their high symmetry and similar NMR spectra (<sup>1</sup>H and <sup>13</sup>C, see the Supporting Information), X-ray crystallo-

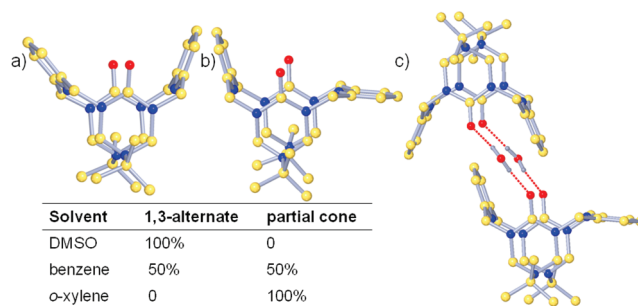


**FIGURE 2.** Comparison of the crystal structures of host **2** obtained via crystallization from DMSO, benzene, and *o*-xylene showing two conformations: (a) the 1,3-alternate conformation was observed in DMSO (oxygen atoms (red), nitrogen (blue), carbon (yellow), hydrogens (omitted)); (b) a partial cone conformer was observed in *o*-xylene; (c) from benzene a 1:1 pair of the two conformations was held together by hydrogen bonds to water.

graphy was used to assign these structures. Dimer **2** crystallized by slow evaporation from several different solvents (~10 mg/mL from benzene, CHCl<sub>3</sub>, DMSO, and xylenes). Its conformation was highly dependent on the crystallization solvent (Figure 2). In general, dimer **2** adopted one of two conformations: the 1,3-alternate conformations (Figure 2a) or the partial cone (Figure 2b). These were similar to what was observed in the case of alkylated calixarenes,<sup>19</sup> however, what was usually one of the least stable conformers, the 1,3-alternate, was observed exclusively in the DMSO crystal structure. In this conformer, the two carbonyl groups were oriented in parallel. One of the pyridyl rings (N4) made an angle of 20.1°, while the other ring (N8) displayed an angle of 40.2° with respect to a plane bisecting the two carbonyl groups. The distance between the pyridyl nitrogen atoms is 4.86 Å. This conformer was further stabilized by weak noncovalent CH...O interactions between the urea carbonyl oxygen and the methyl of DMSO (Supporting Information). In contrast, only the partial cone conformer was observed in the crystals from *o*-xylene (Figure 2b). Here, one of the pyridine rings was flattened, and the (acute) angles are 84.7° (to N4) and 14.8° (to N8), with a distance between pyridyl nitrogen atoms of 4.94 Å.

The crystals of **2** obtained from slow evaporation of benzene displayed both the partial cone and a 1,3-alternate conformation, which were paired 1:1 in the crystals by two water molecules that bridged the carbonyl group through hydrogen bonds (Figure 2c). The water presumably comes from the atmosphere. The presence of both conformers demonstrated the flexibility of the macrocycle and indicated that no one conformer was favored. The hydrogen-bonded dimers were arranged in layers parallel to the crystallographic (011) plane with interstitial benzene molecules positioned between the layers (Supporting Information). Comparison of the three structures of free host **2** showed sometimes formed stabilizing interactions with the urea carbonyl oxygen; however, no interactions were observed between solvent and the pyridine nitrogen. This suggested

(17) Mitchell, A. R.; Pagoria, P. F.; Coon, C. L.; Jessop, E. S.; Poco, J. F.; Tarver, C. M.; Breithaupt, R. D.; Moody, G. L. *Propellants, Explos., Pyrotech.* **1994**, *19*, 232–239.

(18) Shimizu, L. S.; Smith, M. D.; Hughes, A. D.; Shimizu, K. D. *Chem. Commun.* **2001**, 1592–1593.

(19) (a) Macias, A. T.; Norton, J. E.; Evanseck, J. D. *J. Am. Chem. Soc.* **2003**, *125*, 2351–2360. (b) Blixt, J.; Detellier, C. *J. Am. Chem. Soc.* **1994**, *116*, 11957–11960. (c) Harada, T.; Rudzinski, J. M.; Shinkai, S. *J. Chem. Soc., Perkin Trans. 2* **1994**, 2109–2115. (d) van Hoorn, W. P.; Briels, W. J.; van Duynhoven, J. P. M.; van Veggel, F. C. J. M.; Reinhoudt, D. N. *J. Org. Chem.* **1998**, *63*, 1299–1308.

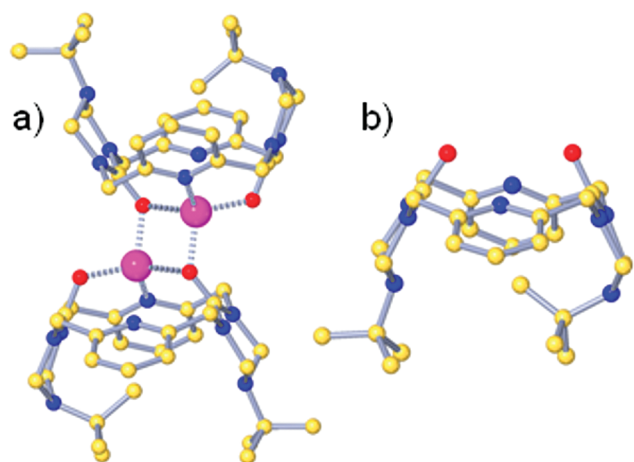


**FIGURE 3.** Views from the X-ray structure of the  $[\text{host } 2 \cdot \text{Li}]_2 \cdot (\text{BF}_4)_2$  complex (oxygen atoms (red), nitrogen (blue), carbon (yellow), hydrogens (omitted), lithium (pink)): (a) ball-and-stick view of the  $[\text{host } 2 \cdot \text{Li}]_2 \cdot (\text{BF}_4)_2$  complex; (b) view of the ligand conformation showing the pyridine nitrogens and the two carbonyl oxygens directed to the same side for cation binding.

that the oxygen was either more basic or more accessible than the pyridine nitrogen.

The change in product distributions when the macrocyclization was carried out with LiH versus NaH, led us to investigate the formation of host·metal complexes. Host **2** was mixed in 1:1 ratio with metal salts ( $\text{LiBF}_4$ ,  $\text{NaBF}_4$ ,  $\text{KBF}_4$ ) and dissolved in acetonitrile (5 mM, 1:1 molar ratio). Slow evaporation methods yielded microcrystals with  $\text{NaBF}_4$  and  $\text{KBF}_4$ . X-ray-quality single crystals were obtained from reaction with  $\text{LiBF}_4$ . The crystal structure revealed the formation of a centrosymmetric dimer with a 2:2 host/ $\text{LiBF}_4$  stoichiometry with the formula  $[\text{2} \cdot \text{Li}]_2 \cdot (\text{BF}_4)_2$ . Host **2** underwent significant conformational adjustment from its unbound state to yield a cone conformation (Figure 3b) that directed the pyridine nitrogens and two carbonyl groups to one face of the macrocycle. Each  $\text{Li}^+$  was coordinated to two urea carbonyl oxygens ( $\text{Li}-\text{O} = 1.898(1) - 1.966(2) \text{ \AA}$ ) and one pyridine nitrogen ( $\text{Li}-\text{N} = 2.141 \text{ \AA}$ ) of one macrocycle as well as to a urea carbonyl of a second macrocycle ( $\text{Li}-\text{O} = 1.908(2) \text{ \AA}$ ). The lithium ions formed shorter interactions with the carbonyl oxygens as compared to the pyridine nitrogens.

Trimer **3** crystallized as a dichloromethane solvate. In the macrocycle, three pyridine nitrogens and one urea carbonyl of triazaninone are facing in the same direction (Figure 4a). The macrocycle did not adopt a planar structure, and none of the rings are parallel. The structure appeared to be flexible enough to fold inward. The pyridine nitrogens adopted a roughly triangular arrangement and their separation distances (3.97, 3.58, and 2.18  $\text{\AA}$ , respectively, accounting for van der Waal radii) roughly defined the interior cavity. The carbonyls did not define a potential binding site for metal cations and were pointed outward.

Host **3** was dissolved in methanol/acetonitrile (5 mM, 1:1 molar ratio) and individually mixed in a 1:1 ratio with the same series of metal salts as well as with  $\text{NaClO}_4$ . Slow evaporation gave crystals of low quality for the  $\text{3} \cdot \text{NaClO}_4$  complex; however, the diffraction data was sufficient to establish general structure connectivity (Figure 4b). Gratifyingly,

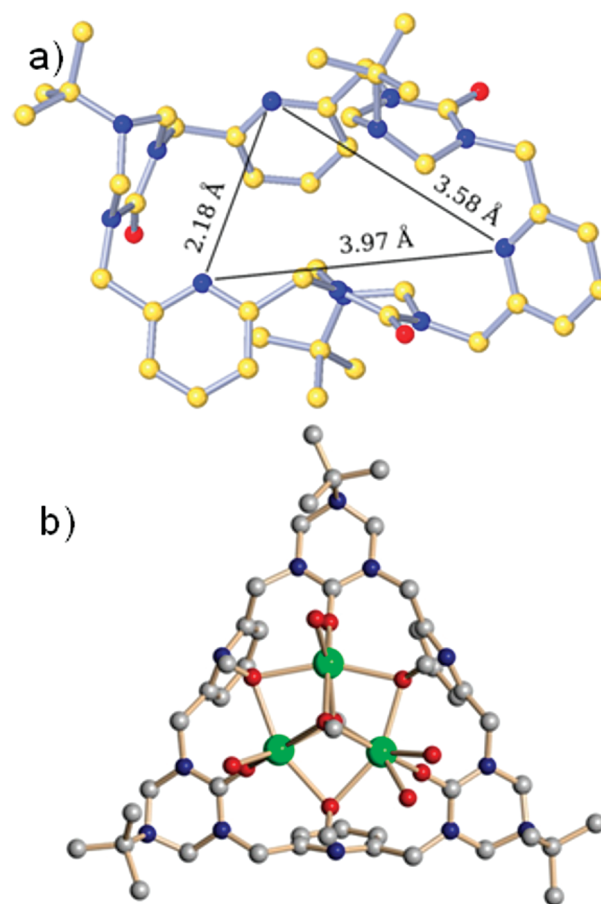


**FIGURE 4.** Comparison of the host **3** and its coordination complex with  $\text{NaClO}_4$ : (a) View of the free host from the X-ray crystal structure of host **3**. Indicated distances are between the van der Waal surfaces of pyridine nitrogens. (b) Low-quality crystals diffracted well enough to establish the general connectivity of the host  $\text{3} \cdot \text{NaClO}_4$  complex in which  $\text{Na}^+$  atoms (green) were coordinated to three carbonyl oxygens as well as to oxygens from perchlorate ions and methanol molecules.

this host was able to accommodate cation guests within its cavity. The structure showed a 1:3 stoichiometry for the host  $\text{3} \cdot \text{NaClO}_4$  complex. The urea carbonyls appear to be a key component for binding the guests and they turned inward to create a complementary endotype binding site for the cations. The  $\text{Na}^+$  atoms were coordinated to three carbonyl oxygens as well as to oxygens from perchlorate ions and methanol molecules. Only the oxygen atoms of the  $\text{ClO}_4$  anions are shown.

Crystals of tetrameric host **4** were obtained by slow evaporation from chloroform. Four urea carbonyls are arranged as up (O1), up (O2), down (O1\*), down (O2\*) arrangement, presumably to minimize dipole interactions. The tetramer molecule was centrosymmetric but not “circular” like other macrocyclic hosts. The large 32-membered macrocycle of host **4** appeared to be much less rigid than the smaller systems and collapsed inward. Figure 5a highlights the elongated ( $\text{N4}-\text{N4}^* \sim 12.56 \text{ \AA}$ ) compact structure formed, which was devoid of open space in its center. This structure suggested that the pyridyl spacers are not rigid enough to define an open cavity. The individual macrocycles lacked noteworthy intermolecular interactions and

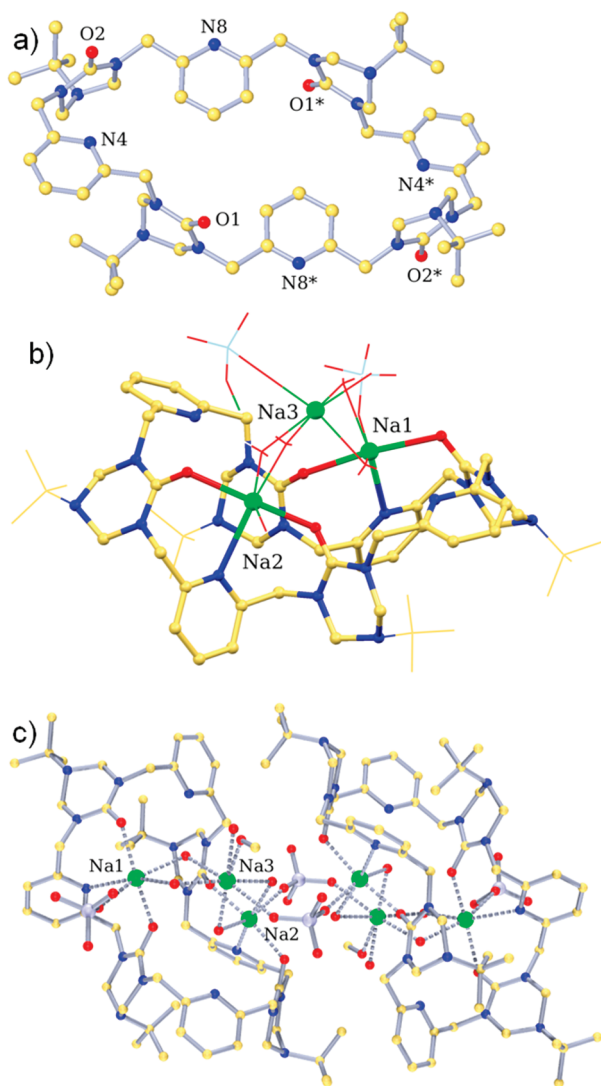


**FIGURE 5.** Views from the X-ray crystal structures of free host **4** and the host **4**·NaClO<sub>4</sub> complex: (a) Top view of free host **4** crystallized from CHCl<sub>3</sub>. Hydrogen atoms and solvent omitted for clarity. (b) Comparison of the binding environment around the sodium ions in the host **4**·Na<sup>+</sup> complex. (c) Structure of the centrosymmetric host **4**·Na<sup>+</sup> dimeric complex bridged by perchlorate anions.

assembled by what was best described as packing via van der Waals interactions.

The host **4**·Na<sup>+</sup> complex was prepared by solvent diffusion method in which the metal salt (NaClO<sub>4</sub>) was dissolved in methanol and layered on the top of a solution of host **4** (10 mg/mL in CHCl<sub>3</sub>). A centrosymmetric, dimeric complex was formed by two bridging perchlorate ions. There were three crystallographically independent sodium atoms and all were six-coordinated (Figure 5b,c). Two sodium atoms (Na1 and Na2) were directly coordinated to the tetramer through two carbonyl oxygen atoms, one pyridyl nitrogen, two bridging water molecules and one perchlorate. Na3 was linked to the 2Na/cycle complex via bridging water molecules.

These solid-state studies demonstrated that each of the hosts could complex alkali metal cations. The smallest host was not able to accommodate the cation within its cavity, while the medium-sized host bound the cation within its

interior. The most flexible host folded to complex these relatively small “hard” cation guests. Both potential ligands (pyridine versus urea) are relatively polarizable and are usually characterized as moderate or soft bases. In all of the complexes, the shorter primary contacts to the cation were formed through the oxygen of the urea carbonyl. The pyridine nitrogens played a supporting role and only sometimes interacted with the cation guests. In all cases where a pyridine nitrogen formed contacts to a cation, its neighboring urea carbonyl oxygen was also involved in an interaction. These results suggest that either the carbonyl oxygen is slightly more basic or the Lewis acid cation is more oxophilic. If we consider the lone-pair cation interaction to be similar to the H-bond interaction, then these observations are consistent with predictions from Hunter that suggest the urea oxygen ( $\beta \sim 8.2$ ) is a better H-bond acceptor than the pyridyl nitrogens ( $\beta \sim 7.2$ ).<sup>20</sup> These predictions are based on flexible systems with single donors and acceptors. In systems with multiple donors and acceptors, the positioning and separation distance are known to affect the strength of these interactions.<sup>21</sup> Ultimately, our goal is to deprotect these macrocycles to the free ureas and to examine their assembly. These models predict that the columnar urea assembly motif should be favored in hosts **2** and **3**, although the pyridine could contribute additional stabilizing interactions. If the urea assembly motif is altered by the close proximity of the pyridine, one could consider new macrocycles that separate these two groups. Larger host **4** is too flexible and is unlikely to self-assemble into columns.

**Solution Studies.** Solid-state studies suggested that these hosts could form complexes with metal salts. We sought next to investigate whether similar complexes were formed in solution and to evaluate the strength and selectivity of these new hosts toward a series of alkali metal salts (LiBF<sub>4</sub>, NaBF<sub>4</sub>, KBF<sub>4</sub>). The tetrafluoroborate salts were used to minimize possible effects by counteranions, which are known to influence the association.<sup>22</sup> <sup>1</sup>H NMR spectroscopy was used to investigate the metal ion binding properties of hosts and to establish the stoichiometry of new host·guest complexes. Both the alkali salts and the hosts displayed good solubility in CD<sub>3</sub>CN at room temperature.

Host **2** was similar in structure to triazinanone macrocycles studied by Dave et al., which displayed conformers that slowly interconvert on the NMR time scale.<sup>23</sup> In the <sup>1</sup>H NMR (CD<sub>3</sub>CN), the 16 methylene protons of host **2** afford four doublets of equal intensity at 5.17, 5.14, 4.37, and 3.88 ppm. COSY and NOE experiments were used to further assign the nonequivalent methylene protons on the

(20) Hunter, C. A. *Angew. Chem., Int. Ed.* **2004**, *43*, 5310–5324.

(21) (a) Jorgensen, W. L.; Pranata, J. *J. Am. Chem. Soc.* **1990**, *112*, 2008–2010. (b) Pranata, J.; Wierschke, S. G.; Jorgensen, W. L. *J. Am. Chem. Soc.* **1991**, *113*, 2810–2819. (c) Murray, T. J.; Zimmerman, S. C. *J. Am. Chem. Soc.* **1992**, *114*, 4010–4011.

(22) (a) Oshovsky, G. V.; Reinhoudt, D. N.; Verboom, W. *Eur. J. Org. Chem.* **2006**, 2810–2816. (b) Shukla, R.; Kida, T.; Smith, B. D. *Org. Lett.* **2000**, *2*, 3099–3102. (c) Pajewski, R.; Ferdani, R.; Pajewska, J.; Li, R. Q.; Gokel, G. W. *J. Am. Chem. Soc.* **2005**, *127*, 18281–18295. (d) Ong, W.; Kaifer, A. E. *J. Org. Chem.* **2004**, *69*, 1383–1385. (e) Huang, F. H.; Jones, J. W.; Slobodnick, C.; Gibson, H. W. *J. Am. Chem. Soc.* **2003**, *125*, 14458–14464. (f) Jones, J. W.; Gibson, H. W. *J. Am. Chem. Soc.* **2003**, *125*, 7001–7004. (g) Bohmer, V.; Dalla, C.; Mandolini, L. *J. Org. Chem.* **2001**, *66*, 1900–1902. (h) Sirish, M.; Schneider, H. *J. Chem. Commun.* **2000**, 23–24. (i) Bartoli, S.; Roelens, S. *J. Am. Chem. Soc.* **1999**, *121*, 11908–11909.

(23) Dave, P. R.; Doyle, G.; Axenrod, T.; Yazdekhashti, H. *J. Org. Chem.* **1995**, *60*, 6946–6952.

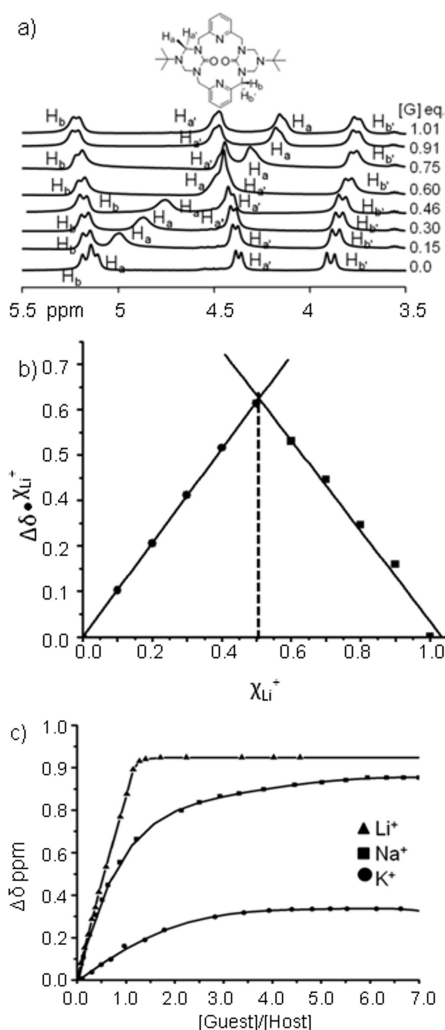


**FIGURE 6.** Host–guest studies with **2** in solution: (a) Partial  $^1\text{H}$  NMR spectrum (400 MHz,  $\text{CD}_3\text{CN}$ ) of host **2** after addition of  $\text{LiBF}_4$  (from bottom to top) 0.00, 0.15, 0.30, 0.46, 0.60, 0.75, 0.91, and 1.01 equiv of  $\text{Li}^+$  ( $[\mathbf{2}] = 5.01 \text{ mM}$ ). The triazinane methylene protons moved upfield with increasing  $\text{Li}^+$  concentrations, a trend that stops after addition of 1 equiv of  $\text{LiBF}_4$ . (b) Job plot for host **2** (10 mM) and  $\text{LiBF}_4$  (10 mM) in  $\text{CD}_3\text{CN}$ . (c)  $^1\text{H}$  NMR chemical shift of host **2** titrated with alkali metal salts ( $\text{LiBF}_4$ ,  $\text{NaBF}_4$ ,  $\text{KBF}_4$ ) at 298 K. Symbols are experimental data points; lines are the best fit curves calculated from nonlinear squares-fitting analysis in  $\text{CD}_3\text{CN}$ . Triazinane methylene protons were monitored after each addition of alkali metal.

triazinanone ring and those adjacent to the pyridine (Supporting Information). Proton NMR studies were performed to further investigate the formation of host/guest complexes in solution. The hosts were titrated with the metal tetrafluoroborate salts while keeping the host concentration constant, and proton NMR spectra were recorded after each addition. Titration of host **2** (5.01 mM) with varying amounts of  $\text{LiBF}_4$  resulted in downfield shifts in the pyridine aromatic resonances by 0.32 ppm; however, the largest shifts were observed for one of the triazinane methylene protons. An expansion of this region of  $^1\text{H}$  NMR spectrum is shown in Figure 6a and displays the shift of this proton, tentatively assigned as the axial proton, from 5.12 to 4.07 ppm. The host/guest stoichiometry was determined using

**TABLE 1.** Association Constants for Complexes of **2–4**,  $\text{CD}_3\text{CN}$ , 25 °C

host	guest metals	stoichiometry (host/guest)	$K_a$ ( $\text{M}^{-1}$ )
<b>2</b>	$\text{LiBF}_4$	1:1	6600
<b>2</b>	$\text{NaBF}_4$	1:1	1500
<b>2</b>	$\text{KBF}_4$	1:1	490
<b>3</b>	$\text{LiBF}_4$	1:1	$10^6$
<b>3</b>	$\text{NaBF}_4$	1:1	1900
<b>3</b>	$\text{KBF}_4$	1:3	$\sim 1500^a$
<b>4</b>	$\text{NaBF}_4$	1:2	2100

<sup>a</sup> $K_a$  was estimated for a 1:1 stoichiometry.

continuous variation (Job plots)<sup>24</sup> at a fixed total concentration of 10 mM. The Job plot showed two lines that intersected at a mole ratio of 0.5, indicating a 1:1 host:guest stoichiometry between host **2** and  $\text{Li}^+$  stoichiometry (Figure 6b). In the solid state, we observed a 2:2 complex for host **2**· $\text{LiBF}_4$ . To investigate if higher order species are present in solution, we plotted the change in chemical shift of the triazinane methylene peak of host **2** as a function of equivalents of  $\text{LiBF}_4$  added (Figure 6c). This showed a clean break at equimolar ratios, which suggested the formation of a stable and discrete 1:1 complex in solution. Given this 1:1 binding model, we estimated the binding constant between host **2** and  $\text{Li}^+$  in  $\text{CD}_3\text{CN}$  with a nonlinear least-squares regression method as  $6600 \text{ M}^{-1}$  (Table 1). Diffusion NMR experiments<sup>25</sup> were performed using a BPP–LED pulse sequence<sup>26</sup> to compare the free host **2** and the host **2**· $\text{Li}^+$  complex (6.3 mM,  $\text{CD}_3\text{CN}$ ). The calculated hydrodynamic radii for the free host **2** and the host **2**· $\text{Li}^+$  complex were similar (6.4 Å vs 6.0 Å), which provided further support for the assignment of a 1:1 stoichiometry in solution in contrast to the 2:2 complex formed in the solid state.

Addition of tetrafluoroborate salts of sodium and potassium to host **2** resulted in similar trends, although the upfield shifts were not as large. The absolute magnitude of the maximum chemical shifts decreased in the order of  $\text{Li}^+ > \text{Na}^+ > \text{K}^+$ . Job plots of both  $\text{NaBF}_4$  and  $\text{KBF}_4$  with host **2** indicated a 1:1 host:guest stoichiometry (Supporting Information), although the plot of the change in chemical shift as a function of equivalents of tetrafluoroborate salt added was more gradual with no break at 1 equiv of guest (Figure 6c). This suggested that host **2** had a much lower association constant with these cations and also indicated that stoichiometries other than 1:1 were possible. Assuming a 1:1 binding stoichiometry, we estimated the binding constant between host **2** and  $\text{Na}^+$  with a nonlinear least-squares regression method as  $1500 \text{ M}^{-1}$  with host **2** showing the lowest affinity for  $\text{K}^+$  ( $K_a \sim 490 \text{ M}^{-1}$ ). The observed affinity of host **2** for cations ( $\text{Li}^+ > \text{Na}^+ > \text{K}^+$ ) was a little surprising given the relatively soft nature of the urea carbonyl oxygen versus the harder  $\text{Li}^+$  cation. We therefore sought to investigate if this propensity for binding the smaller, harder cation was carried through this structurally similar series of hosts.

Given synthetic observations that the base  $\text{LiH}$  afforded host **3** as the major product, we expected this host to display higher affinity for  $\text{Li}^+$  in solution. Indeed, the crystal

(24) Hirose, K. *J. Inclusion Phenom. Macrocyclic Chem.* **2001**, *39*, 193–209.

(25) (a) Antalek, B. *Concepts Magn. Reson.* **2002**, *14*, 225–258. (b) Pelta, M. D.; Barjat, H.; Morris, G. A.; Davis, A. L.; Hammond, S. J. *Magn. Reson. Chem.* **1998**, *36*, 706–714.

(26) Wu, D. H.; Chen, A. D.; Johnson, C. S. *J. Magn. Reson. Ser. A* **1995**, *115*, 260–264.

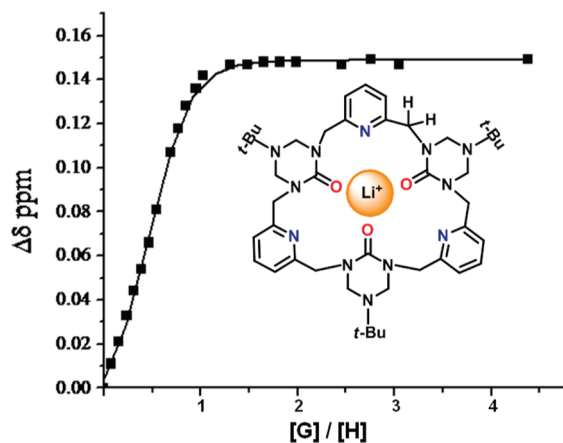


**FIGURE 7.** Complexation-induced shifts during the  $^1\text{H}$  NMR titration. ( $[G]$  = concentration of guest  $\text{Li}^+$ ,  $\Delta\delta$  = chemical shift change of the indicated host **3** methylene protons,  $[3] = 2.09$  mM). Symbols are experimental data points; line is the best fit curve calculated from nonlinear square fitting analysis in  $\text{CD}_3\text{CN}$ . A possible structure of the complex formed by host **3** and  $\text{Li}^+$  was suggested.

structure of a host **3**· $\text{NaClO}_4$  complex suggested that this host could orient its three carbonyl oxygens as well as the three pyridine nitrogens inward, potentially affording a hexadentate ligand. Upon addition of  $\text{LiBF}_4$  to host **3**, the signal due to methylene protons neighboring the pyridine rings moved downfield by 0.15 ppm and broaden. Figure 7 plotted the change in shift of the bridged  $-\text{CH}_2$  protons as a function of  $\text{Li}^+$  concentration and showed a sharp break at equimolar concentrations. Both the fitting of titration data and the mole ratio plots indicated the formation of complex with 1:1 binding stoichiometry. A nonlinear least-squares regression method gave an estimated association constant of  $9.5 \times 10^5 \text{ M}^{-1}$  ( $K_a$ ) for host **3**· $\text{Li}^+$ , which was at the limit of what can be determined by NMR. We turned to diffusion NMR experiments<sup>25</sup> using a BPP-LED pulse sequence<sup>26</sup> to further probe the free host, free guest, and a 1:1 host/guest (10 mM,  $\text{CD}_3\text{CN}$ ) solution. The calculated hydrodynamic radii of the **3**· $\text{Li}^+$  complex was larger than the free host (10 Å vs 8.4 Å), and a similar experiment using lithium NMR gave an identical calculated hydrodynamic radii for the complex (Supporting Information). Further studies using lithium diffusion NMR detected no free or unbound  $\text{Li}^+$  in the 1:1 host:guest solution. Taken together the NMR titration data and the diffusion NMR studies suggested that host **3** and  $\text{Li}^+$  form a strong and stable complex in solution.

Titration of host **3** with  $\text{NaBF}_4$  or  $\text{KBF}_4$  produced smaller shifts in the same methylene region. The Job plot indicated that  $\text{NaBF}_4$  formed a 1:1 complex with host **3** with a significantly smaller association constant ( $K_a \sim 1900 \text{ M}^{-1}$ ) while  $\text{KBF}_4$  formed a 1:3 complex with host **3** with yet lower affinity. The Job plots for these salts displayed more scatter leaving open the possibility of multiple complex stoichiometries. These studies demonstrated that host **3** had a high affinity for the harder lithium ion versus sodium or potassium. Given X-ray structure evidence that carbonyl oxygens that are primarily responsible for binding, we suggested a structure of this complex in Figure 7. We are currently working on methods for growing X-ray quality crystals of the host **3**· $\text{Li}$  complex to confirm the structure and are also screening other metal salts as guests for this host.

The large flexible host **4** showed no response to  $\text{LiBF}_4$  or  $\text{KBF}_4$  in solution; however, upon addition of  $\text{NaBF}_4$  the signal due to methylene protons in **4** neighboring the pyridine rings moved downfield by 0.16 ppm (Supporting Information). A continuous variation (Job) plot of host **4** with  $\text{NaBF}_4$  at a fixed concentration of 10 mM displayed two lines that intersected at a guest mole fraction of 0.6, suggesting a 1:2 stoichiometry (host/guest). This is consistent with observations from the crystal structure of host **4**· $\text{NaClO}_4$  complex in which two sodium atoms were directly coordinated to a single host. Addition of an aqueous  $\text{NaClO}_4$  solution to the crude mixture of hosts **2–4** afforded the precipitation of the host **4**· $\text{NaClO}_4$  complex after overnight stirring, experimentally suggesting that host **4** had a high affinity for sodium. We are currently evaluating cations and small molecule guests that have sizes more complementary to the larger cavity of this host.

In summary, we synthesized three macrocyclic hosts containing varying numbers of pyridines and protected urea groups. These hosts showed affinity for alkali metal salts of lithium, sodium, and potassium. Comparisons of the X-ray crystal structures of the free hosts and their host–guest complexes suggested that these macrocyclic hosts were flexible enough to adjust their conformations to accommodate cations. These structures showed that the urea carbonyl oxygen formed the most important interactions with the alkali metal cations, experimentally indicating that the oxygen was the more basic site. However, neighboring pyridine nitrogen contributed additional stabilizing interactions. Solution studies revealed that host **3** was selective for  $\text{Li}^+$  and bound this cation with high affinity in acetonitrile. In comparison, host **2** displayed a moderate preference for the lithium cation, while host **4** favored complexes with sodium salts.

These results suggest that upon deprotection to the free urea the urea carbonyl should be the best H-bond acceptor. Therefore, we predict that the smaller macrocycles **2** and **3** should assemble primarily through the typical urea assembly motif, although the proximity of the pyridine nitrogen may affect the assembly. It remains to be seen if these additional interactions would alter the three-dimensional structure. The flexibility of host **4** combined with our observations that cations interacted with both the pyridine nitrogen and the carbonyl oxygen, leads us to predict that this macrocycle may be more promiscuous in its assembly patterns. For such a host, the pyridine nitrogens may need to be masked perhaps through interaction with a supramolecular protecting group or an azophilic guest that might selectively interact with the pyridine lone pair. A potential choice for this guest would include alcohols or phenols, which are not as good H-bond donors as the urea NHs. We are now focused on studying assembly of the free urea analogues of these hosts in the presence and absence of guests.

## Experimental Section

**Synthesis of Triazinanone-Protected Bis-urea Macrocycle (2–4).** A suspension of 5-*tert*-butyltetrahydro-1,3,5-triazin-2(1*H*)-one (1.00 g, 6.4 mmol) and NaH (460 mg, 19.2 mmol) in THF (300 mL) was heated under reflux for 1 h and then allowed to cool to room temperature. A solution of 2,6-bis-(bromomethyl)pyridine (1.69 g, 6.4 mmol) in THF (150 mL) was added dropwise over a 60 min period. The resulting mixture was

heated under reflux for 48 h. Then it was allowed to cool to room temperature, and ice-cold water (200 mL) was added carefully to destroy excess NaH. After removal of the THF in vacuo, the aqueous mixture was extracted with CH<sub>2</sub>Cl<sub>2</sub> (3 × 100 mL). The combined organic layers were washed with water (2 × 25 mL), dried with MgSO<sub>4</sub>, and evaporated under reduced pressure. Silica gel chromatography (CHCl<sub>3</sub>/MeOH 9:1) of the residue afforded macrocycles **2–4** in the elute order of **4** (0.31 g, 19%), **3** (0.13 g, 8.0%), and **2** (0.5 g, 30%).

**Dimer 2:** <sup>1</sup>H NMR (400 MHz, DMSO-*d*<sub>6</sub>, δ), 7.54 (t, *J* = 7.6 Hz, 2H), 7.02 (d, *J* = 7.6 Hz, 4H), 5.1 (d, *J* = 11.6 Hz, 4H), 5.01 (d, *J* = 16.4 Hz, 4H), 4.35 (d, *J* = 11.6 Hz, 4H), 3.92 (d, *J* = 16.4 Hz, 4H), 1.18 (s, 18H). <sup>13</sup>C NMR (100.56 MHz, DMSO-*d*<sub>6</sub>, δ) 158.7, 154.5, 136.2, 119.5, 64.4, 53.7, 49.8, 28.6. Mp 237–240 °C; HRMS (ESI) calcd for C<sub>28</sub>H<sub>41</sub>N<sub>8</sub>O<sub>2</sub> (MH<sup>+</sup>) 521.3352, found 521.3351.

**Trimer 3:** <sup>1</sup>H NMR (400 MHz, CDCl<sub>3</sub>, δ), 7.52 (t, *J* = 7.8 Hz, 3H), 7.15 (d, *J* = 7.5 Hz, 6H), 4.53 (s, 12H), 4.28 (s, 12H), 1.12 (m, 27H); <sup>13</sup>C NMR (100.56 MHz, CDCl<sub>3</sub>, δ) 157.43, 156.40, 137.64, 121.25, 63.34, 54.38, 50.92, 29.00; mp 286–289 °C; HRMS (ESI) calcd for C<sub>42</sub>H<sub>61</sub>N<sub>12</sub>O<sub>3</sub> (MH<sup>+</sup>) 781.4989, found 781.4982.

**Tetramer 4:** <sup>1</sup>H NMR (400 MHz, CDCl<sub>3</sub>, δ) 7.61 (t, *J* = 7.8 Hz, 4H), 7.25 (d, *J* = 7.5 Hz, 8H), 4.62 (s, 16H), 4.41 (s, 16H), 1.08 (m, 36H); <sup>13</sup>C NMR (CDCl<sub>3</sub>, 100.56 MHz, δ) 157.80, 156.35, 137.70, 120.90, 63.27, 54.49, 51.10, 28.81; mp 298–301 °C; HRMS (ESI) calcd for C<sub>56</sub>H<sub>81</sub>N<sub>16</sub>O<sub>4</sub> (MH<sup>+</sup>) 1041.6626, found 1041.6605.

**Determination of association constants by NMR.** Solutions of host (**2–4**) were prepared in 2 mL volumetric flasks. The solid compounds were placed directly into the flask, and CD<sub>3</sub>CN was added to the mark. The solution was stirred for several hours to ensure that all components were dissolved. This host solution (1 mL) was used for the preparation of guest solution (metal salt) in separate 1 mL volumetric flasks. Fresh host solution (600 μL) was transferred to NMR tube, and a spectrum was recorded at room temperature. Then aliquots of alkali metal salt were added to host solution. Guest solution was added until the guest concentration reached 7 times that of host concentration. The

chemical shifts of the methylene protons were recorded after each addition of guest solution. The association constants were determined by nonlinear least-squares fitting analysis of the titration curve for 1:1 and 1:2 binding. The chemical shift changes under fast exchange condition can be written as follows:

$$\delta = \delta_1 - \left( \frac{\delta_1 - \delta_C}{2[\mathbf{1}]_0} \right) (B - \sqrt{B^2 - 4[\mathbf{M}]_0[\mathbf{1}]_0}) \quad (1)$$

Here, δ is the observed chemical shift, δ<sub>1</sub> is the chemical shift for the free host, δ<sub>C</sub> is the chemical shift for the complex, [1]<sub>0</sub> is the initial concentration of host, and [M]<sub>0</sub> is the initial concentration of the metal ion.

$$B = [\mathbf{M}]_0 + \frac{1}{K_a} + [\mathbf{1}]_0 \quad (2)$$

Figure 6c show typical plots of the observed and calculated titration curves obtained by this method for all alkali metal salts.

**Job Plot.** Complexation stoichiometry was determined by a Job plot using <sup>1</sup>H NMR spectroscopy.<sup>24</sup> Stock solutions of host (20 mM) and guest (20 mM) in CD<sub>3</sub>CN were prepared. Ten NMR spectra were obtained in the following volume ratios (host/guest): 600:0, 540:60, 480:120, 420:180, 360:240, 300:300, 240:360, 180:420, 120:480, 60:540 (μL/μL). The chemical shift of methylene protons were recorded for each sample, the corresponding concentration of complex was determined for each sample, and the Job plot was obtained by plotting complex concentration as a function of the mole fraction of alkali metal ions.

**Acknowledgment.** We gratefully acknowledge support in part for this work from the NSF (CHE-0718171 and CHE-1012298) and from the University of South Carolina Nanocenter.

**Supporting Information Available:** <sup>1</sup>H and <sup>13</sup>C NMR spectra of all new compounds, X-ray crystallographic files (CIF) for hosts **2–4** and their complexes, <sup>1</sup>H NMR titration of **1–3**, and diffusion NMR studies. This material is available free of charge via the Internet at <http://pubs.acs.org>.